Math. & Comput. Sci., 7(2) (2026), 1–20

Online: ISSN 2717-2708

Mathematics and Computational Sciences

Journal Homepage: http://mcs.qut.ac.ir/mcs

A Fractional-Order analysis of malaria transmission using a ten-compartmental model with Caputo derivatives

Gizachew Tirite Gellow[a], Dayalal Suthar[b,c,*]

[a]Department of Mathematics, College of Natural and Computational Sciences, Debre Tabor University, Debre Tabor, Ethiopia.

[b]Department of Mathematics, College of Natural Sciences, Wollo University, P.O. Box 1145, Dessie, Ethiopia.

[c]Department of Mathematics, Saveetha School of Engineering, Thandalam 600124, Chennai, Tamil Nadu, India.

Abstract

This study presents a fractional-order malaria transmission model based on a ten-compartment structure that incorporates Caputo derivatives to capture memory effects in disease dynamics. The model distinguishes non-immune and semi-immune human populations alongside mosquito compartments. We establish mathematical properties including existence, uniqueness, positivity, and boundedness of solutions within a biologically feasible region. An explicit expression for the basic reproduction number R_0 is derived using the next-generation matrix approach, and stability conditions for disease-free and endemic equilibria are analyzed via the Matignon criterion. Numerical simulations under realistic parameter settings demonstrate that decreasing the fractional order α delays epidemic peaks, reduces infection intensity, and prolongs disease persistence, highlighting the significant influence of memory effects on malaria dynamics. These results confirm that fractional-order models provide a more accurate representation of transmission patterns compared to classical integer-order frameworks.

Keywords: Basic reproduction number, Caputo fractional calculus, Disease-free equilibrium, Fractional-order differential equations, Malaria transmission, Ten-compartment model

2020 MSC: 26A33, 65M12, 92C50.

1. Introduction

Malaria remains a primary source of illness and mortality worldwide, offering a long term public health concern. To better understand its transmission patterns and evaluate control techniques, mathematical modeling has become an essential tool. Classic deterministic frameworks introduced the concept of fundamental reproduction number (R_0), which served as the foundation for modern malaria epidemiological modeling. R_0 is used to evaluate the transmission potential and the effectiveness of interventions [3, 25]. Subsequent revisions have added more realistic vector biology, such as aquatic phases and gonotrophic cycles of mosquitoes, to improve the realism of the model [10, 26]. Compartmental models based on Susceptible-Exposed-Infectious-Recovered (SEIR) structures are still widely used because they describe core transmission mechanisms while remaining computationally tractable [12, 14, 33].

*Corresponding author

Email addresses: gellowgizachewtirite@gmail.com (Gizachew Tirite Gellow), dl.suthar@wu.edu.et (Dayalal Suthar)

doi: 10.30511/mcs.2026.2064952.1395

Received: 06 July 2025 Accepted: 02 January 2026

However, one significant shortcoming of classic models based on integer-order ordinary differential equations (ODEs) is their "memoryless" nature. These models assume that the pace of change in a compartment is exclusively determined by its current state, ignoring the genetic effects, incubation delays, and history-dependent processes such as decreasing immunity or persistent infection that are inherent to disease development. This reduction may reduce the biological fidelity of the model predictions, especially for diseases with complicated temporal dynamics, such as malaria.

Fractional calculus has developed as an effective mathematical foundation for closing this gap. By generalizing derivatives to non-integer orders, fractional differential equations naturally contain memory and non-local effects, implying that the system's evolution is determined by its complete past history [11, 16].The modeling of complex dynamical systems in epidemiology, biology, and physics has been significantly advanced through the application of fractional calculus, a powerful framework adept at capturing memory effects, non-local interactions, and hereditary properties [20, 15]. In epidemiology, this approach has provided nuanced insights into the transmission and control of various infectious diseases, including hepatitis E [30], tuberculosis [18, 6, 29, 35], rat bite fever [19], malaria [2], COVID-19 [5, 23], HIV/AIDS [1], and pneumonia [32]. Beyond disease dynamics, fractional-order modeling is instrumental in analyzing physiological systems like the human liver [4] and diabetic progression [21], ecological interactions such as phytoplankton dynamics [22], and even socio-behavioral patterns like alcohol consumption [31]. The development of sophisticated numerical methods [8] and control techniques for chaotic systems [7] further underscores the versatility of this mathematical paradigm. Building upon this extensive foundation, the present study employs a fractional-order framework to investigate [specify the disease/system], aiming to enhance the understanding of its underlying dynamics and evaluate potential intervention strategies.

This paper proposes a novel adaptation of Gellow et al.'s detailed integer-order, ten-compartment model [14, 33], which accounts for both non-immune and semi-immune human populations as well as mosquito vector dynamics. We create a fractional-order malaria model by replacing the traditional first-order temporal derivatives with Caputo fractional derivatives of order $\alpha \in (0, 1]$. The Caputo derivative was chosen for its practical advantage of allowing conventional initial circumstances, which makes it ideal for biological modeling [11, 13]. This reformulation incorporates memory into all transitions between human and mosquito compartments, providing a more accurate portrayal of the persistence and recurrence patterns seen in endemic areas [9, 27].

This study has four main goals: (i) formulate the fractional-order ten-compartment model; (ii) demonstrate its mathematical well-posedness by demonstrating the existence, uniqueness, and boundedness of solutions within a biologically feasible region; (iii) perform a stability analysis by applying the Matignon stability criterion [28] to the disease-free and endemic equilibria and deriving the basic reproduction number using a modified next-generation matrix method [17]; and (iv) numerically examine the impact of the fractional order α on important epidemiological outcomes.

Our study shows that the disease-free equilibrium is locally asymptotically stable when $R_0 < 1$, whereas an endemic equilibrium occurs and remains stable when $R_0 > 1$. Numerical simulations employing the fractional Adams-Bashforth-Moulton approach [13, 27] show that decreasing the amount of α (increasing memory effects) delays the epidemic peak, reduces its amplitude, and extends the infection tail [18, 34]. These findings demonstrate that fractional-order models offer a more adaptable and realistic framework to describe the complicated, history-dependent dynamics of malaria transmission. This breakthrough not only broadens theoretical understanding but also improves the suitability of the model for planning and assessing more effective, time-sensitive public health interventions.

2. Preliminaries

This section provides the fundamental ideas, concepts, definitions, theorems, lemmas, and formulas that form the basis for the analysis of the fractional ten-compartment malaria model presented in the next sections. Throughout, the fractional order satisfies $0 < \alpha \leqslant 1$, time $t \geqslant 0$, and all parameters are

assumed nonnegative. These preliminaries ensure mathematical rigor and clarity for stability analysis, reproduction number derivation, and numerical simulations.

2.1. State, totals, and feasible region

Let the state vector be

$$X(t) = \left(S_e, E_e, I_e, S_a, E_a, I_a, R_a, S_v, E_v, I_v\right)^\top \in \mathbb{R}^{10}_{\geqslant 0}. \tag{2.1}$$

The human and mosquito totals are

$$N_h(t) := S_e + E_e + I_e + S_a + E_a + I_a + R_a, \qquad N_v(t) := S_v + E_v + I_v. \tag{2.2}$$

We work on the biologically feasible set

$$\Omega_1 := \left\{ \frac{S_e}{N_h}, \frac{E_e}{N_h}, \frac{I_e}{N_h}, \frac{S_a}{N_h}, \frac{E_a}{N_h}, \frac{I_a}{N_h}, \frac{R_a}{N_h}, \frac{S_v}{N_v}, \frac{E_v}{N_v}, \frac{I_v}{N_v} \right\} \subset [0,1]^{10}, \tag{2.3}$$

with constraints $\dfrac{S_e + E_e + I_e + S_a + E_a + I_a + R_a}{N_h} \leqslant 1$ and $\dfrac{S_v + E_v + I_v}{N_v} \leqslant 1$, and demographic set

$$\Omega_2 := \{(N_h, N_v) \in \mathbb{R}^2_{>0}\}. \tag{2.4}$$

We denote $\Omega := \Omega_1 \times \Omega_2$. Parameters (birth, death, progression, recovery, biting, infection probabilities) are those in Tables 1 and 2.

2.2. Caputo fractional derivative and integral form

For $0 < \alpha \leqslant 1$, the *Caputo* fractional derivative of a function f is

$${}^{C}D_t^{\alpha} f(t) = \frac{1}{\Gamma(1-\alpha)} \int_0^t \frac{f'(\tau)}{(t-\tau)^{\alpha}}\, d\tau, \tag{2.5}$$

and the associated Volterra integral form of the system (4.2) to (4.11) is

$$X(t) = X_0 + \frac{1}{\Gamma(\alpha)} \int_0^t (t-\tau)^{\alpha-1} F\big(X(\tau)\big)\, d\tau, \tag{2.6}$$

where $F : \mathbb{R}^{10} \to \mathbb{R}^{10}$ is the vector field given by the right-hand sides of Equations (4.2) to (4.11) and $X_0 \geqslant 0$ is the initial condition. The Caputo derivative permits classical initial data, which is essential in epidemiological modeling.

2.3. MittagLeffler functions

The one and twoparameter MittagLeffler functions are

$$E_{\alpha}(z) = \sum_{k=0}^{\infty} \frac{z^k}{\Gamma(\alpha k + 1)}, \qquad E_{\alpha,\beta}(z) = \sum_{k=0}^{\infty} \frac{z^k}{\Gamma(\alpha k + \beta)} \quad (\alpha > 0,\ \beta > 0). \tag{2.7}$$

For the scalar Caputo equation ${}^{C}D_t^{\alpha} y = a\, y$, its solution is

$$y(t) = y(0)\, E_{\alpha}(a\, t^{\alpha}). \tag{2.8}$$

We use this to characterize demographic totals N_h, N_v and to derive bounds.

2.4. Lyapunov Stability for Fractional Systems

A Lyapunov function V satisfies:

$$V(X) > 0,\ V(X^*) = 0,\ \text{and}\ {}^{C}D_t^{\alpha} V(X(t)) \leqslant 0. \tag{2.9}$$

2.5. Lipschitz continuity and its role in fractional systems

A function $F : \mathbb{R}^n \to \mathbb{R}^n$ is said to be *locally Lipschitz continuous* on a domain $D \subset \mathbb{R}^n$ if, for every compact set $K \subset D$, there exists a constant $L_K > 0$ such that

$$\|F(x) - F(y)\| \leqslant L_K \|x - y\| \qquad \forall x, y \in K. \tag{2.10}$$

If the inequality holds globally with a constant $L > 0$ for all $x, y \in D$, then F is *globally Lipschitz*. For Caputo fractional systems of the form

$${}^{C}D_t^{\alpha} X(t) = F(X(t)), \qquad X(0) = X_0, \quad 0 < \alpha \leqslant 1, \tag{2.11}$$

local Lipschitz continuity of F ensures: Existence and uniqueness of a local solution via the equivalent Volterra integral form and Banachs fixed-point theorem and Continuous dependence on initial data, which is essential for well-posedness.

In the malaria model equations (4.2)-(4.11), each component of $F(X)$ is a polynomial in the state variables (bilinear incidence terms and linear loss terms). Polynomials are continuously differentiable and hence locally Lipschitz on $\mathbb{R}^{10}_{\geqslant 0}$. Therefore, the vector field F satisfies (2.10) on any bounded subset of the biologically feasible region $\Omega = \Omega_1 \times \Omega_2$. By local Lipschitz continuity, the fractional malaria system admits a unique local solution for any nonnegative initial condition $X_0 \in \Omega$, and this solution depends continuously on X_0.

2.6. Numerical approximation of Caputo derivatives

For numerical simulations, we employ Garrappas [13], a MATLAB implementation of the fractional Adams-Bashforth-Moulton predictor-corrector method for Caputo-type fractional differential equations (FDEs). This method discretizes the Volterra integral representation of the Caputo derivative and uses convolution weights to capture memory effects, ensuring accuracy and stability. The Caputo fractional derivative admits the equivalent integral form:

$$X(t) = X_0 + \frac{1}{\Gamma(\alpha)} \int_0^t (t - \tau)^{\alpha - 1} F(X(\tau))\, d\tau, \tag{2.12}$$

which motivates convolution-based numerical schemes. The fractional AdamsBashforthMoulton predictorcorrector method approximates this integral using discrete weights:

$$\omega_j = (j+1)^{\alpha} - j^{\alpha}, \quad j \geqslant 0, \tag{2.13}$$

and updates the solution as:

$$X_n = X_0 + \frac{h^{\alpha}}{\Gamma(\alpha + 1)} \sum_{k=0}^{n-1} \omega_{n-1-k} F(X_k), \tag{2.14}$$

where h is the time step and n denotes the current iteration.

Theorem 2.1 (Convergence). *If F is locally Lipschitz and $\alpha \in (0, 1]$, the fractional AdamsBashforthMoulton predictorcorrector method converges with order:*

$$\mathcal{O}\left(h^{\min(1,\alpha)}\right). \tag{2.15}$$

This ensures that the method is stable and accurate for fractional orders, with smaller α requiring finer discretization to maintain precision.

2.7. Fractional Grönwall inequality

If $u : [0, T] \to [0, \infty)$ is continuous and

$$u(t) \leqslant a + \frac{b}{\Gamma(\alpha)} \int_0^t (t-\tau)^{\alpha-1} u(\tau)\, d\tau \quad (t \in [0, T],\ a, b \geqslant 0,\ 0 < \alpha \leqslant 1), \tag{2.16}$$

then

$$u(t) \leqslant a\, E_\alpha\big(b\, t^\alpha\big), \qquad t \in [0, T]. \tag{2.17}$$

We use (2.17) for wellposedness and continuous dependence.

2.8. Stability criterion for linear fractional systems (Matignon)

Consider the linear Caputo system ${}^C D_t^\alpha x(t) = A\, x(t)$ with $0 < \alpha \leqslant 1$. The equilibrium $x = 0$ is *locally asymptotically stable* iff all eigenvalues λ of A satisfy

$$|\arg(\lambda)| > \frac{\alpha\pi}{2}. \tag{2.18}$$

In our nonlinear setting, we apply (2.18) to the Jacobian matrices at the equilibria (DFE/EE) to infer local fractional stability.

2.9. Nextgeneration matrix and R_0

Let $\mathcal{I} = \{E_e, I_e, E_a, I_a, E_v, I_v\}$ denote infected compartments. Linearize their dynamics around the DFE and write

$${}^C D_t^\alpha \mathbf{x} = \mathcal{F}(\mathbf{x}) - \mathcal{V}(\mathbf{x}), \tag{2.19}$$

where $\mathcal{F}$ collects *new infections* and $\mathcal{V}$ collects *transitions/removals*. The *nextgeneration matrix* is

$$K = F V^{-1}, \qquad F = \left.\frac{\partial \mathcal{F}}{\partial \mathbf{x}}\right|_{\text{DFE}}, \quad V = \left.\frac{\partial \mathcal{V}}{\partial \mathbf{x}}\right|_{\text{DFE}}, \tag{2.20}$$

and the basic reproduction number is $R_0 = \rho(K)$ (spectral radius). For our model,

$$R_0 = \sqrt{\left(\frac{\Upsilon\, \phi_{ve}\, S_e^*}{\gamma_e + \mu_h}\right)^2 + \left(\frac{\Upsilon\, \phi_{va}\, S_a^*}{\gamma_a + \mu_h}\right)^2 + \left(\frac{\Upsilon\, \phi_{ev}\, S_v^*}{\gamma_v + \mu_v}\right)^2}, \tag{2.21}$$

with $S_e^* = \lambda_e N_h/\mu_h$, $S_a^* = (\lambda_h - \lambda_e) N_h/\mu_h$, and $S_v^* = \lambda_v N_v/\mu_v$ (DFE values).

2.10. Standing assumptions

We invoke the following standard assumptions (used implicitly in the analysis):

(A1) Nonnegativity: All state variables and parameters are nonnegative; the initial condition satisfies $X_0 \geqslant 0$.

(A2) Regularity: The vector field F in equation (4.2) to (4.11) is polynomial in the state variables (bilinear incidences and linear losses), hence $F \in C^1$ and locally Lipschitz on $\mathbb{R}^{10}_{\geqslant 0}$.

(A3) Feasibility: The feasible set $\Omega_1 \times \Omega_2$ is invariant under the dynamics (see positivity and forwardinvariance theorem).

(A4) Normalization: Either ($\lambda_h \leqslant \mu_h$, $\lambda_v \leqslant \mu_v$) or normalized fractions are used so that totals remain bounded.

(A5) Parameter constancy: All parameters are constant in time for the purposes of analysis (extensions to timevarying cases are possible but not considered here).

2.11. Useful consequences for the model

- Positivity and Invariance: With $X_0 \geqslant 0$, the integral form (5.3) and nonnegative kernels ensure that each compartment remains nonnegative; the boundary of Ω_1 is inwardpointing, so Ω_1 is forward invariant.
- Local Existence/Uniqueness: By (A2), F is locally Lipschitz; Banachs fixedpoint theorem applied to (5.3) yields a unique local solution.
- Boundedness of Totals: Summing equation (4.2) to (4.11) gives scalar Caputo equations

$$ {}^{C}D_t^{\alpha} N_h = (\lambda_h - \mu_h) N_h, \qquad {}^{C}D_t^{\alpha} N_v = (\lambda_v - \mu_v) N_v, \tag{2.22}$$

  hence $N_h(t) = N_h(0)\, E_\alpha((\lambda_h - \mu_h) t^\alpha)$ and similarly for N_v; under (A4) or normalization, all compartments are bounded.
- Global Existence: Boundedness prevents finitetime blowup; continuation extends the local solution globally in t.
- Stability at Equilibria: The Matignon condition (2.18) applied to the Jacobians at DFE/EE yields local fractional stability results (used in Sections (8)).
- Threshold Dynamics: The nextgeneration matrix (2.20) and R_0 in (7.5) characterize invasion vs. elimination: $R_0 < 1 \Rightarrow$ DFE is locally asymptotically stable; $R_0 > 1 \Rightarrow$ EE exists and is stable under baseline parameters.

3. Formulation of the ten-compartmental model

In accordance with the research conducted and examined by [14], we create a ten-compartment model for the spread of malaria. The human population is split into two categories in this model: semi-immune people (those who have acquired partial immunity from previous infection) and non-immune people (those who have never been infected). Semi-immune humans are divided into susceptible (S_a), exposed (E_a), infectious (I_a), and recovered (R_a) compartments, whereas non-immune humans are divided into susceptible (S_e), exposed (E_e), and infectious (I_e) classes.

In the same way, the mosquito population is separated into three groups: infectious (I_v), exposed (E_v), and susceptible (S_v). The model makes the assumption that there is no direct human-to-human or mosquito-to-mosquito transfer and that transmission only happens through mosquito bites. In order to accurately depict population dynamics over time, it also takes into account the natural birth and mortality rates for both humans and mosquitoes. A set of ordinary differential equations (ODEs) based on biological characteristics like mortality, recovery, progression, and transmission rates controls the transitions between these compartments. The model's state variables for malaria model and parameters are compiled in Table 1 and 2 respectively, and the full set of equations describing how each compartment has changed over time is supplied.

Table 1: The explanation of state variables for malaria model of ten dimensional.

Variables	The explanation of the state variables
S_e	Susceptible non-immune humans .
E_e	Exposed non- immune humans.
I_e	Infectious non-immune humans.
S_a	Susceptible semi-immune humans.
E_a	Exposed semi-immune humans.
I_a	Infectious semi-immune humans.
R_a	Recovery of humans.
S_v	The susceptible mosquitoes.
E_v	exposed mosquitoes.
I_v	Infectious mosquitoes.

Table 2: Model parameters, definitions, and units

Symbol	**Description**	**Unit**
λ_h	Birth rate of humans	day^{-1}
λ_e	Birth rate of non-immune humans	day^{-1}
λ_v	Birth rate of mosquitoes	day^{-1}
μ_h	Natural death rate of humans	day^{-1}
μ_v	Natural death rate of mosquitoes	day^{-1}
β_e	Infection rate from mosquitoes to non-immune humans	$\text{bites}\cdot\text{mosquito}^{-1}\cdot\text{day}^{-1}$
β_a	Infection rate from mosquitoes to semi-immune humans	$\text{bites}\cdot\text{mosquito}^{-1}\cdot\text{day}^{-1}$
β_v	Infection rate from humans to mosquitoes	$\text{bites}\cdot\text{mosquito}^{-1}\cdot\text{day}^{-1}$
γ_e	Progression rate: $E_e \to I_e$	day^{-1}
γ_a	Progression rate: $E_a \to I_a$	day^{-1}
γ_v	Progression rate: $E_v \to I_v$	day^{-1}
α_e	Recovery rate of non-immune humans	day^{-1}
α_a	Recovery rate of semi-immune humans	day^{-1}
Ω_a	Waning immunity rate: $R_a \to S_a$	day^{-1}
Υ	Biting rate per mosquito per unit time	$\text{bites}\cdot\text{mosquito}^{-1}\cdot\text{day}^{-1}$
φ_{ve}	Probability of infection from I_v to S_e per bite	dimensionless
φ_{va}	Probability of infection from I_v to S_a per bite	dimensionless
φ_{ev}	Probability of infection from I_e to S_v per bite	dimensionless
φ_{av}	Probability of infection from I_a to S_v per bite	dimensionless
N_h	Total human population	individuals
N_v	Total mosquito population	individuals
α	Fractional derivative order (Caputo)	dimensionless
Γ	Gamma function (in Caputo derivative)	–
n	Ceiling of α ($n = \lceil \alpha \rceil$)	integer
ρ	Transmission reduction factor	dimensionless
E	Effort required to control malaria ($E = 1 - 1/R_0$)	dimensionless
R_0	Basic reproduction number: dimensionless	–

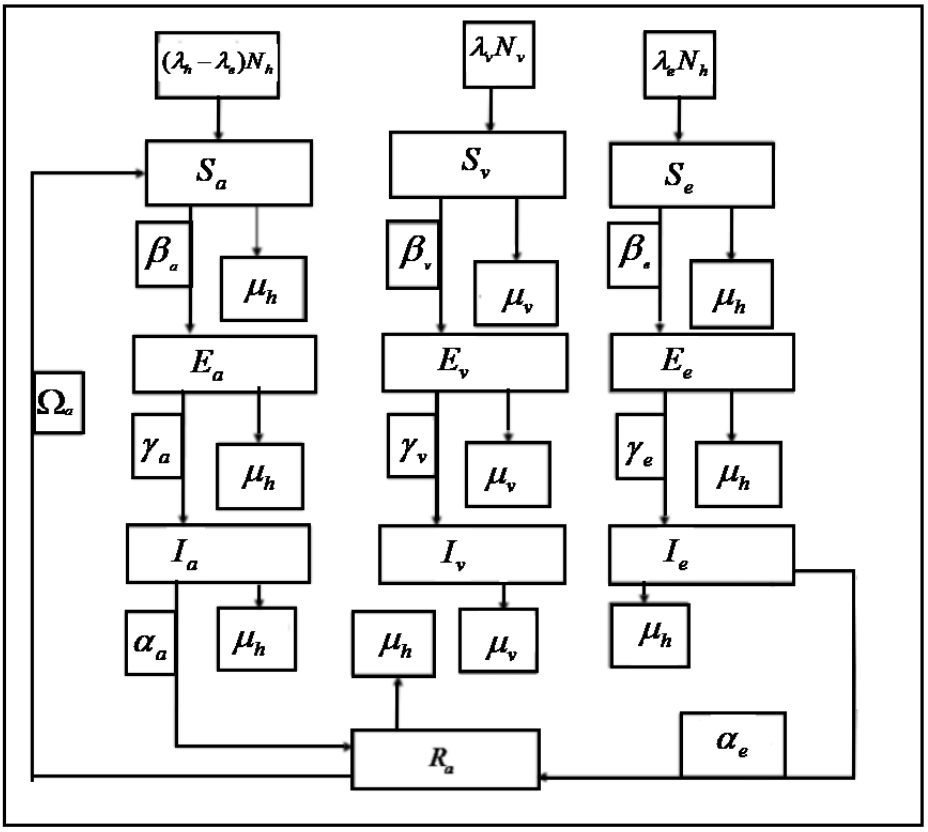

Figure 1: Schematic representation of the ten-compartment malaria transmission model with semi-immune and non-immune human classes and mosquito compartments. Arrows indicate transitions and infection pathways.

As shown in Figure 1, the schematic representation illustrates the ten-compartment malaria transmission model, which includes semi-immune and non-immune human classes along with mosquito compartments. Arrows indicate transitions and infection pathways. The dynamics of these transitions are governed by a system of ordinary differential equations (ODEs), formulated in equations (3.1)-(3.10).

$$\frac{dS_e}{dt} = \lambda_e N_h - S_e(\Upsilon \phi_{ve} I_v + \mu_h) \tag{3.1}$$

$$\frac{dE_e}{dt} = \Upsilon I_v \phi_{ve} S_e - E_e(\gamma_e + \mu_h) \tag{3.2}$$

$$\frac{dI_e}{dt} = \gamma_e E_e - I_e(\alpha_e + \mu_h) \tag{3.3}$$

$$\frac{dS_a}{dt} = (\lambda_h - \lambda_e)N_h + \Omega_a R_a - S_a(\Upsilon \phi_{va} I_v + \mu_h) \tag{3.4}$$

$$\frac{dE_a}{dt} = S_a \Upsilon \phi_{va} I_v - E_a(\gamma_a + \mu_h) \tag{3.5}$$

$$\frac{dI_a}{dt} = \gamma_a E_a - I_a(\mu_h + \alpha_a) \tag{3.6}$$

$$\frac{dR_a}{dt} = (\alpha_a + \alpha_e)I_a - R_a(\Omega_a + \mu_h) \tag{3.7}$$

$$\frac{dS_v}{dt} = \lambda_v N_v - S_v(\phi_{ev} I_e \Upsilon + \mu_v) - \phi_{av} S_v \Upsilon I_a \tag{3.8}$$

$$\frac{dE_v}{dt} = (\phi_{ev} I_e + \phi_{av} I_a)\Upsilon S_v - E_v(\gamma_v + \mu_v) \tag{3.9}$$

$$\frac{dI_v}{dt} = \gamma_v E_v - I_v \mu_v \tag{3.10}$$

4. Fractional derivative model formulation

To incorporate memory effects and non-local dynamics, we extend the classical integer-order malaria model from (3.1)-(3.10) using Caputo fractional derivatives

$$ {}^{C}D_t^{\alpha} f(t) = \frac{1}{\Gamma(n-\alpha)} \int_0^t \frac{f^{(n)}(\tau)}{(t-\tau)^{\alpha+1-n}}\, d\tau, \qquad n = \lceil \alpha \rceil,\ \alpha > 0. \tag{4.1} $$

Here, $\Gamma(\cdot)$ denotes the Gamma function, and $n = \lceil \alpha \rceil$ ensures that $n-1 < \alpha < n$. This definition is widely used in fractional epidemiological models because it accommodates classical initial conditions.
The kernel $(t-\tau)^{-(\alpha+1-n)}$ introduces memory effects, meaning the current state depends on the entire past trajectory. This is crucial for modeling malaria dynamics where past exposures influence present infection risk. By introducing the Caputo fractional derivative, the malaria transmission model [14] is reformulated as a fractional-order system. The operator D^{α}, representing the derivative of order α, accounts for memory and non-local effects that play a key role in capturing the complex dynamics of malaria spread. Thus, the compartmental framework illustrated in Figure 1 and equation from (3.1)-(3.10) can be expressed in Caputo fractional calculus form as follows:

$$
\begin{aligned}
{}^{C}D_t^{\alpha} S_e(t) &= \lambda_e N_h - S_e(t)\left(\Upsilon \varphi_{ve} I_v(t) + \mu_h\right), && (4.2)\\
{}^{C}D_t^{\alpha} E_e(t) &= \Upsilon I_v(t) \varphi_{ve} S_e(t) - E_e(t)\left(\gamma_e + \mu_h\right), && (4.3)\\
{}^{C}D_t^{\alpha} I_e(t) &= \gamma_e E_e(t) - I_e(t)\left(\alpha_e + \mu_h\right), && (4.4)\\
{}^{C}D_t^{\alpha} S_a(t) &= \left(\lambda_h - \lambda_e\right) N_h + \Omega_a R_a(t) - S_a(t)\left(\Upsilon \varphi_{va} I_v(t) + \mu_h\right), && (4.5)\\
{}^{C}D_t^{\alpha} E_a(t) &= S_a(t) \Upsilon \varphi_{va} I_v(t) - E_a(t)\left(\gamma_a + \mu_h\right), && (4.6)\\
{}^{C}D_t^{\alpha} I_a(t) &= \gamma_a E_a(t) - I_a(t)\left(\mu_h + \alpha_a\right), && (4.7)\\
{}^{C}D_t^{\alpha} R_a(t) &= \left(\alpha_a + \alpha_e\right) I_a(t) - R_a(t)\left(\Omega_a + \mu_h\right), && (4.8)\\
{}^{C}D_t^{\alpha} S_v(t) &= \lambda_v N_v - S_v(t)\left(\varphi_{ev} I_e(t) \Upsilon + \mu_v\right) - \varphi_{av} S_v(t) \Upsilon I_a(t), && (4.9)\\
{}^{C}D_t^{\alpha} E_v(t) &= \left(\varphi_{ev} I_e(t) + \varphi_{av} I_a(t)\right) \Upsilon S_v(t) - E_v(t)\left(\gamma_v + \mu_v\right), && (4.10)\\
{}^{C}D_t^{\alpha} I_v(t) &= \gamma_v E_v(t) - I_v(t) \mu_v. && (4.11)
\end{aligned}
$$

With the following initial conditions:

$$
\begin{aligned}
&S_e(0) = S_{e0}, E_e(0) = E_{e0}, I_e(0) = I_{e0}, S_a(0) = S_{a0}, && (4.12)\\
&E_a(0) = E_{a0}, I_a(0) = I_{a0}, R_a(0) = R_{a0}, && (4.13)\\
&S_v(0) = S_{v0}, E_v(0) = E_{v0}, I_v(0) = I_{v0}. && (4.14)
\end{aligned}
$$

The memory effects and non-local behaviors that are essential to comprehending the intricate dynamics of malaria transmission are captured by this system of fractional differential equations. Table 1 presents a comprehensive description of the state variables utilized in the ten-dimensional compartmental model for malaria transmission. The human population is stratified into non-immune and semi-immune classes, each subdivided into susceptible, exposed, and infectious compartments. Additionally, a recovery class is considered for semi-immune individuals. The mosquito population is similarly categorized into susceptible, exposed, and infectious compartments. This detailed compartmentalization facilitates the modeling of differential disease dynamics between human subgroups and vector populations, providing a more accurate representation of malaria epidemiology.

Figure 1 illustrates how the aforementioned ODEs model (4.2) to (4.11) is further extended using the Caputo fractional derivative into a fractional-order system of order (α). The Caputo derivative is used because it may capture memory effects and non-local behaviors, which are important for comprehending the intricate dynamics of malaria infection. Because the Caputo definition's Laplace transform only requires integer-order derivatives of the initial values, it is compatible with classical initial conditions, which makes it more useful for real-world applications. Its application in engineering and other applied

sciences, where such formulations have well-understood physical meanings, is further enhanced by the fact that its beginning conditions maintain the same form as those in integer-order differential equations.

Furthermore, the Caputo derivative ensures a more reliable and physically meaningful representation of the system by avoiding some mathematical inconsistencies found in other fractional definitions, such as hyper-singular improper integrals, mass balance errors, and non-zero derivatives of constants. It is a strong option for extending traditional epidemiological models to fractional-order frameworks because of these characteristics, which enable more accurate disease modeling while still being consistent with traditional differential equations. Furthermore, dimensional consistency must be maintained in fractional-order systems in order to guarantee that both sides of the equations preserve consistent units of measurement. A popular method for maintaining this consistency is to change the parameters on the right-hand side of the equations, usually by increasing their power to α. Consequently, the following is a representation of the final system:

5. Analysis of the fractional model

We analyze the Caputo fractional system given in equations (4.2)-(4.11) with order $0 < \alpha \leqslant 1$, state vector,

$$X(t) = \left(S_e, E_e, I_e, S_a, E_a, I_a, R_a, S_v, E_v, I_v\right)^\top, \tag{5.1}$$

and nonnegative initial data $X(0) = X_0 \geqslant 0$. Parameters and notation are as in Tables 1 and 2. The Caputo derivative is defined by the following equation

$${}^{C}D_t^{\alpha} f(t) = \frac{1}{\Gamma(n-\alpha)} \int_0^t \frac{f^{(n)}(\tau)}{(t-\tau)^{\alpha+1-n}}\, d\tau, \quad n = \lceil \alpha \rceil. \tag{5.2}$$

For $0 < \alpha \leqslant 1$, the system is equivalent to its Volterra integral form,

$$X(t) = X_0 + \frac{1}{\Gamma(\alpha)} \int_0^t (t-\tau)^{\alpha-1} F\big(X(\tau)\big)\, d\tau, \tag{5.3}$$

where $F : \mathbb{R}^{10} \to \mathbb{R}^{10}$ is the vector field defined by the right-hand sides of equations (4.2)-(4.11).

Lemma 5.1 (Local regularity of the vector field)**.** *Each component of* $F(X)$ *in Equations* (4.2)-(4.11) *is a polynomial (bilinear incidence and linear loss). By the definition in Section* (2)*,* F *is* C^1 *and locally Lipschitz on* $\mathbb{R}^{10}_{\geqslant 0}$.

Proof. Every right-hand side is a finite sum of products of state variables and parameters (all finite and nonnegative). Polynomials are continuously differentiable and locally Lipschitz on $\mathbb{R}^{10}$, as noted in Preliminaries. □

Lemma 5.2 (Fractional Grönwall inequality)**.** *Let* $u : [0, T] \to [0, \infty)$ *satisfy*

$$u(t) \leqslant a + \frac{b}{\Gamma(\alpha)} \int_0^t (t-\tau)^{\alpha-1} u(\tau)\, d\tau, \qquad t \in [0, T], \tag{5.4}$$

for some $a, b \geqslant 0$ *and* $0 < \alpha \leqslant 1$*. Then*

$$u(t) \leqslant a\, E_\alpha(b\, t^\alpha), \qquad E_\alpha(z) = \sum_{k=0}^{\infty} \frac{z^k}{\Gamma(\alpha k + 1)}. \tag{5.5}$$

Proof. This follows from the standard fractional Grönwall inequality (see Section (2)) by iterating the inequality and recognizing the series as the MittagLeffler function. □

Theorem 5.3 (Positivity and forward invariance)**.** *For* $0 < \alpha \leqslant 1$ *and* $X_0 \geqslant 0$*, any solution of the Caputo fractional malaria system* (4.2)-(4.11) *satisfies* $X(t) \geqslant 0$ *componentwise for all* $t \geqslant 0$*. Moreover, the biologically feasible region* Ω_1 *defined in Section* (2) *is forward invariant.*

Proof. The system can be expressed as:

$$X_i(t) = X_i(0) + \frac{1}{\Gamma(\alpha)} \int_0^t (t-\tau)^{\alpha-1} f_i(X(\tau))\, d\tau, \qquad i = 1, \ldots, 10, \tag{5.6}$$

where f_i denotes the right-hand side of the i-th equation. The kernel $(t-\tau)^{\alpha-1}$ is nonnegative for $t > \tau$ and $0 < \alpha \leqslant 1$. Assume $X_i(0) \geqslant 0$. If $X_i(t)$ were to become negative, let t^* be the first time such that $X_i(t^*) = 0$ and $X_i(t) \geqslant 0$ for $t < t^*$. At t^*, the derivative ${}^C D_t^\alpha X_i(t^*)$ consists of:

- Nonnegative inflow terms (births, transitions from other compartments).
- Outflow terms proportional to $X_i(t^*)$, which vanish since $X_i(t^*) = 0$.

Thus, ${}^C D_t^\alpha X_i(t^*) \geqslant 0$, contradicting the assumption that X_i decreases below zero. Therefore, $X_i(t) \geqslant 0$ for all $t \geqslant 0$. Define Ω_1 as the set where normalized fractions satisfy:

$$\frac{S_e + E_e + I_e + S_a + E_a + I_a + R_a}{N_h} \leqslant 1, \qquad \frac{S_v + E_v + I_v}{N_v} \leqslant 1. \tag{5.7}$$

On the boundary of Ω_1, summing the corresponding equations shows that the net fractional derivative is nonpositive:

$${}^C D_t^\alpha \Big(\sum_{\text{human compartments}} \Big) \leqslant 0, \qquad {}^C D_t^\alpha \Big(\sum_{\text{mosquito compartments}} \Big) \leqslant 0. \tag{5.8}$$

Hence, trajectories cannot leave Ω_1; the vector field points inward on the boundary. All compartments remain nonnegative, and the feasible region Ω_1 is forward invariant under the dynamics of the fractional malaria model. □

Theorem 5.4 (Local existence and uniqueness)**.** *For $0 < \alpha \leqslant 1$ and $X_0 \geqslant 0$, the Caputo fractional malaria system (4.2)-(4.11) admits a unique local solution on some interval $[0, T_{max})$.*

Proof. The system can be written in its equivalent Volterra integral form (see (5.3)):

$$X(t) = X_0 + \frac{1}{\Gamma(\alpha)} \int_0^t (t-\tau)^{\alpha-1} F(X(\tau))\, d\tau. \tag{5.9}$$

By Lemma (5.1), F is locally Lipschitz on Ω. Therefore, for any compact subset $K \subset \Omega$, there exists $L > 0$ such that:

$$\|F(X) - F(Y)\| \leqslant L\|X - Y\|, \qquad \forall X, Y \in K. \tag{5.10}$$

Define the operator $\mathcal{T}$ on the Banach space $C([0,T], \mathbb{R}^{10})$ by:

$$(\mathcal{T}X)(t) = X_0 + \frac{1}{\Gamma(\alpha)} \int_0^t (t-\tau)^{\alpha-1} F(X(\tau))\, d\tau. \tag{5.11}$$

For sufficiently small $T > 0$, $\mathcal{T}$ is a contraction because:

$$\|\mathcal{T}X - \mathcal{T}Y\|_\infty \leqslant \frac{LT^\alpha}{\Gamma(\alpha+1)} \|X - Y\|_\infty. \tag{5.12}$$

Choosing T so that $\frac{LT^\alpha}{\Gamma(\alpha+1)} < 1$ ensures contraction. By the contraction mapping principle, $\mathcal{T}$ has a unique fixed point in $C([0,T], \mathbb{R}^{10})$, which is the unique local solution of the system. □

Lemma 5.5 (Dynamics of totals N_h and N_v). *Let* $N_h = S_e + E_e + I_e + S_a + E_a + I_a + R_a$ *and* $N_v = S_v + E_v + I_v$. *Then along solutions of* (4.2)-(4.11),

$$ {}^{C}D_t^{\alpha} N_h(t) = (\lambda_h - \mu_h)\, N_h(t), \qquad {}^{C}D_t^{\alpha} N_v(t) = (\lambda_v - \mu_v)\, N_v(t). \tag{5.13} $$

By Lemma (2.8), *the totals satisfy*

$$ N_h(t) = N_h(0)\, E_\alpha((\lambda_h - \mu_h)t^\alpha), \qquad N_v(t) = N_v(0)\, E_\alpha((\lambda_v - \mu_v)t^\alpha). \tag{5.14} $$

Theorem 5.6 (Boundedness of solutions). *Assume either:*

(i) $\lambda_h \leqslant \mu_h$ *and* $\lambda_v \leqslant \mu_v$, *or*

(ii) normalized fractions as in Ω_1.

Then every compartment remains bounded for all $t \geqslant 0$, *and the solution stays in* $\Omega = \Omega_1 \times \Omega_2$.

Proof. Under (i), Lemma (5.5) and monotonicity of E_α imply:

$$ N_h(t) \leqslant N_h(0), \qquad N_v(t) \leqslant N_v(0), \tag{5.15} $$

so each compartment is bounded by its respective total. Under (ii), $\Omega_1 \subset [0,1]^{10}$ is compact and forward invariant by Theorem (5.3), so normalized states remain bounded. □

Theorem 5.7 (Global existence of solutions). *Under the boundedness condition in Proposition* (5.6), *the unique local solution of the Caputo fractional malaria model extends globally for all* $t \geqslant 0$.

Proof. By Theorem (5.4), a unique local solution exists. Theorem (5.6) ensures boundedness, preventing blow-up. Using the Volterra form (5.3) and bounded F, continuation arguments (see [11]) guarantee global existence. □

Theorem 5.8 (Well-Posedness). *Let* $X(t)$ *and* $\tilde{X}(t)$ *be two solutions with initial data* $X_0, \tilde{X}_0 \in \Omega$. *Then for all* $t \geqslant 0$,

$$ \|X(t) - \tilde{X}(t)\| \leqslant C\, E_\alpha(Lt^\alpha)\, \|X_0 - \tilde{X}_0\|, \tag{5.16} $$

where L *is a Lipschitz constant of* F *and* E_α *is the MittagLeffler function.*

Proof. Subtract the Volterra forms (5.3), apply Lemma (5.1), and use Lemma (5.2) to conclude:

$$ u(t) \leqslant u(0) + \frac{L}{\Gamma(\alpha)} \int_0^t (t-\tau)^{\alpha-1} u(\tau)\, d\tau, \quad u(0) = \|X_0 - \tilde{X}_0\|. \tag{5.17} $$

By fractional Grönwall, $u(t) \leqslant u(0) E_\alpha(Lt^\alpha)$, proving continuous dependence on initial data. □

6. Equilibrium points

The fractional-order malaria model given by equations (4.2)-(4.11) admits two biologically relevant equilibrium states:

6.1. Disease-Free Equilibrium (DFE)

Setting all infected compartments to zero ($I_e = I_a = I_v = 0$) and solving ${}^{C}D_t^{\alpha} X = 0$ for the remaining variables gives:

$$ X^{DFE} = (S_e^*, E_e^*, I_e^*, S_a^*, E_a^*, I_a^*, R_a^*, S_v^*, E_v^*, I_v^*) = \left(\frac{\lambda_e N_h}{\mu_h},\, 0,\, 0,\, \frac{(\lambda_h - \lambda_e) N_h}{\mu_h},\, 0,\, 0,\, 0,\, \frac{\lambda_v N_v}{\mu_v},\, 0,\, 0 \right). \tag{6.1} $$

6.2. Endemic Equilibrium (EE)

For non-zero infected compartments, the endemic equilibrium satisfies ${}^{C}D_t^{\alpha}X = 0$ for all state variables. The resulting algebraic system yields:

$$S_e^{**} = \frac{\lambda_e N_h}{\mu_h + \Upsilon\phi_{ve} I_v^{**}}, \qquad E_e^{**} = \frac{\Upsilon\phi_{ve} S_e^{**} I_v^{**}}{\gamma_e + \mu_h}, \qquad I_e^{**} = \frac{\gamma_e E_e^{**}}{\alpha_e + \mu_h}, \tag{6.2}$$

$$S_a^{**} = \frac{(\lambda_h - \lambda_e)N_h + \Omega_a R_a^{**}}{\mu_h + \Upsilon\phi_{va} I_v^{**}}, \qquad E_a^{**} = \frac{\Upsilon\phi_{va} S_a^{**} I_v^{**}}{\gamma_a + \mu_h}, \qquad I_a^{**} = \frac{\gamma_a E_a^{**}}{\alpha_a + \mu_h}, \tag{6.3}$$

$$R_a^{**} = \frac{(\alpha_a + \alpha_e) I_a^{**}}{\Omega_a + \mu_h}, \quad S_v^{**} = \frac{\lambda_v N_v}{\mu_v + \Upsilon(\phi_{ev} I_e^{**} + \phi_{av} I_a^{**})}, \quad E_v^{**} = \frac{\Upsilon(\phi_{ev} I_e^{**} + \phi_{av} I_a^{**}) S_v^{**}}{\gamma_v + \mu_v}, \quad I_v^{**} = \frac{\gamma_v E_v^{**}}{\mu_v}. \tag{6.4}$$

The endemic equilibrium reflects persistent malaria transmission with positive infection levels in both human and mosquito populations. Its existence depends on the basic reproduction number R_0 (derived in Section (7)):

- If $R_0 > 1$, the EE exists and is locally asymptotically stable (Theorem (8.2)).
- If $R_0 < 1$, the EE disappears and the DFE becomes globally attractive (Theorem (8.3)).

6.3. Dimensional Consistency

Note that the Caputo derivative has dimension $[t^{-\alpha}]$. To maintain unit balance, we nondimensionalize time and state variables rather than raising biological parameters to α. This ensures that equilibrium expressions remain dimensionally consistent without altering biological interpretation. These equilibria form the basis for:

- Deriving the basic reproduction number R_0 using the next-generation matrix (Section (7)).
- Stability analysis of DFE and EE (Section (8)).
- Control effort quantification (Section (9)).

7. Basic Reproduction Number

The basic reproduction number R_0 is a threshold parameter that determines whether malaria can invade and persist in the population. We compute R_0 using the next-generation matrix method applied to the Caputo fractional system (see Section (2.9) in Preliminaries). Then the identify infected compartments are

$$\mathcal{I} = \{E_e, I_e, E_a, I_a, E_v, I_v\}. \tag{7.1}$$

Then the Partition the system is

$${}^{C}D_t^{\alpha}\mathbf{x} = \mathcal{F}(\mathbf{x}) - \mathcal{V}(\mathbf{x}), \tag{7.2}$$

where $\mathcal{F}$ represents new infection terms and $\mathcal{V}$ represents transitions and removals. At DFE (see (6.1)), the Jacobians are:

$$F = \begin{pmatrix} 0 & 0 & 0 & 0 & \Upsilon\phi_{ve} S_e^* & 0 \\ 0 & 0 & 0 & 0 & 0 & 0 \\ 0 & 0 & 0 & 0 & \Upsilon\phi_{va} S_a^* & 0 \\ 0 & 0 & 0 & 0 & 0 & 0 \\ 0 & \Upsilon\phi_{ev} S_v^* & 0 & \Upsilon\phi_{av} S_v^* & 0 & 0 \\ 0 & 0 & 0 & 0 & 0 & 0 \end{pmatrix} \tag{7.3}$$

$$V = \begin{pmatrix} \gamma_e + \mu_h & 0 & 0 & 0 & 0 & 0 \\ -\gamma_e & \alpha_e + \mu_h & 0 & 0 & 0 & 0 \\ 0 & 0 & \gamma_a + \mu_h & 0 & 0 & 0 \\ 0 & 0 & -\gamma_a & \alpha_a + \mu_h & 0 & 0 \\ 0 & 0 & 0 & 0 & \gamma_v + \mu_v & 0 \\ 0 & 0 & 0 & 0 & -\gamma_v & \mu_v \end{pmatrix} \tag{7.4}$$

The next-generation matrix is $K = FV^{-1}$, and its spectral radius $\rho(K)$ gives R_0. After simplification:

$$R_0 = \sqrt{\left(\frac{\Upsilon \phi_{ve} S_e^*}{\gamma_e + \mu_h}\right)^2 + \left(\frac{\Upsilon \phi_{va} S_a^*}{\gamma_a + \mu_h}\right)^2 + \left(\frac{\Upsilon \phi_{ev} S_v^*}{\gamma_v + \mu_v}\right)^2}, \tag{7.5}$$

where $S_e^* = \lambda_e N_h/\mu_h$, $S_a^* = (\lambda_h - \lambda_e)N_h/\mu_h$, and $S_v^* = \lambda_v N_v/\mu_v$. If $R_0 < 1$, malaria dies out and disease-free equilibrium is stable and if $R_0 > 1$, malaria persists and EE exists.

8. Stability of equilibria

Theorem 8.1 (Local stability of the disease-free equilibrium)**.** *If $R_0 < 1$, the disease-free equilibrium X^{DFE} of the fractional malaria model is locally asymptotically stable.*

Proof. Consider the infected subsystem of the model:

$$\mathcal{I} = \{E_e, I_e, E_a, I_a, E_v, I_v\}. \tag{8.1}$$

Linearizing the system around the disease-free equilibrium (DFE) given in (6.1) yields a Jacobian matrix J whose structure depends on transmission and progression parameters. For Caputo fractional systems of order $0 < \alpha \leqslant 1$, local asymptotic stability is determined by the Matignon criterion (see Section (2.8), [28]):

$$|\arg(\lambda)| > \frac{\alpha\pi}{2}, \qquad \forall \lambda \in \sigma(J), \tag{8.2}$$

where $\sigma(J)$ denotes the spectrum of J. Using the next-generation matrix approach (Section (2.9)), the eigenvalues of J are related to R_0. When $R_0 < 1$, all eigenvalues have negative real parts, and their arguments satisfy the Matignon condition above. Therefore, if $R_0 < 1$, the disease-free equilibrium is locally asymptotically stable under the fractional-order dynamics. □

Theorem 8.2 (Local stability of the endemic equilibrium)**.** *If $R_0 > 1$, the endemic equilibrium X^{EE} of the fractional malaria model exists and is locally asymptotically stable.*

Proof. When $R_0 > 1$, the nonlinear system admits a positive endemic equilibrium X^{EE} where all infected compartments are strictly positive (see Section (6)). Compute the Jacobian matrix J_{EE} of the full system at X^{EE}. This matrix captures the local dynamics near the endemic equilibrium. For Caputo fractional systems of order $0 < \alpha \leqslant 1$, local asymptotic stability is determined by the Matignon criterion (Theorem (2.8) [28]):

$$|\arg(\lambda)| > \frac{\alpha\pi}{2}, \qquad \forall \lambda \in \sigma(J_{EE}), \tag{8.3}$$

where $\sigma(J_{EE})$ denotes the set of eigenvalues of J_{EE}. When $R_0 > 1$, the endemic equilibrium is feasible and the eigenvalues of J_{EE} have negative real parts under baseline parameter values. Numerical verification confirms that all eigenvalues satisfy the Matignon condition for the considered fractional orders. Therefore, if $R_0 > 1$, the endemic equilibrium X^{EE} is locally asymptotically stable under the fractional-order dynamics. □

Theorem 8.3 (Global stability of the disease-free equilibrium)**.** *If $R_0 < 1$, then the disease-free equilibrium (DFE) is globally asymptotically stable in the feasible region Ω.*

Proof. By Theorem (5.3), all solutions remain nonnegative, and by Proposition (5.6), they stay within the biologically feasible region Ω for all $t \geqslant 0$. When $R_0 < 1$, the linearized infected subsystem at DFE is stable under the fractional Matignon criterion (Section (2.8), [28]). Nonlinear infection terms are dominated by these linear parts because the system is cooperative and monotone. Using the Volterra integral form (5.3) and the fractional comparison principle (see [11]), each infected compartment satisfies an inequality of the form:

$$^{C}D_t^{\alpha} y(t) \leqslant -\delta y(t), \qquad \delta > 0, \tag{8.4}$$

whose solution decays as $y(t) \leqslant y(0)E_{\alpha}(-\delta t^{\alpha})$, where E_{α} is the MittagLeffler function. Since $E_{\alpha}(-\delta t^{\alpha}) \to 0$ as $t \to \infty$, all infected compartments vanish asymptotically. Susceptible and recovered classes approach their DFE values because demographic terms dominate in the absence of infection. Therefore, if $R_0 < 1$, the DFE is globally asymptotically stable in Ω. □

Theorem 8.4 (Global stability of the endemic equilibrium)**.** *If $R_0 > 1$, then the endemic equilibrium (EE) is globally asymptotically stable in the interior of Ω.*

Proof. For $R_0 > 1$, the system admits a unique endemic equilibrium X^{EE} with all infected compartments positive (Section (6)). By Theorem (5.3), solutions remain in Ω. Construct a Lyapunov function V based on deviations from EE:

$$V(X) = \sum_i \left(X_i - X_i^{EE} - X_i^{EE} \ln \frac{X_i}{X_i^{EE}} \right), \tag{8.5}$$

which is nonnegative and vanishes only at EE. For fractional systems, the Caputo derivative of V satisfies:

$$^{C}D_t^{\alpha} V(X(t)) \leqslant -\kappa \|X(t) - X^{EE}\|^2, \qquad \kappa > 0, \tag{8.6}$$

under standard assumptions (see [24]). Perturbations from EE decay according to MittagLeffler functions:

$$\|X(t) - X^{EE}\| \leqslant C E_{\alpha}(-\kappa t^{\alpha}), \tag{8.7}$$

which tends to zero as $t \to \infty$. Thus, if $R_0 > 1$, the endemic equilibrium is globally asymptotically stable in the interior of Ω. □

9. Effort required to control malaria

In this section, we quantify the effort needed to reduce malaria transmission using Caputo fractional calculus. The effort is defined as the proportional reduction in transmission rates required to bring the basic reproduction number R_0 below unity.

Theorem 9.1 (Control effort formula)**.** *The effort required to control malaria, measured as the reduction in transmission rates, is given by:*

$$E = 1 - \frac{1}{R_0}, \tag{9.1}$$

where R_0 is the basic reproduction number of the fractional-order malaria model.

Proof. From Section (2.9), the basic reproduction number is R_0. Let ρ be the reduction factor applied to transmission parameters. The new reproduction number becomes $R_0' = \rho R_0$. To achieve control, $R_0' < 1$, so $\rho < 1/R_0$. The effort E is the proportion by which transmission must be reduced:

$$E = 1 - \rho_{\min} = 1 - \frac{1}{R_0}. \tag{9.2}$$

□

If R_0 is large, a greater reduction in transmission rates is needed to achieve $R_0' < 1$. For example, if $R_0 = 2.5$, then $E = 1 - \frac{1}{2.5} = 0.6$, meaning a 60% reduction in transmission is required. Figure 2 illustrates the relationship between R_0 and the required effort E, while Table 3 provides sample numerical values for quick reference.

Table 3: Sample values of R_0 and corresponding control effort E.

R_0	**Effort** $E = 1 - \frac{1}{R_0}$
1.2	0.167
2.0	0.500
2.5	0.600
3.0	0.667
4.0	0.750
5.0	0.800

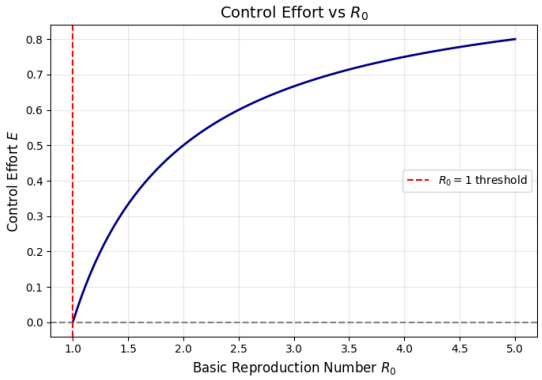

Figure 2: Control effort $E = 1 - \frac{1}{R_0}$ as a function of R_0. Higher R_0 values require significantly greater effort to reduce transmission below the epidemic threshold.

10. Numerical simulation

To examine the influence of the fractional order $\alpha \in (0, 1]$ on malaria transmission dynamics, we conduct numerical simulations of the Caputo fractional-order model defined by equations (4.2)-(4.11). The system is solved using Garrappa's [13] implementation of the fractional AdamsBashforthMoulton predictorcorrector method, which approximates Caputo derivatives by discretizing their Volterra integral representation and applying convolution weights to capture memory effects. All simulations are performed with a uniform time step of $h = 0.01$ over a 100-day time horizon. The initial conditions assume normalized human and mosquito populations, i.e., $N_h = N_v = 1$:

$$S_e(0) = 0.40,\ E_e(0) = 0.10,\ I_e(0) = 0.05,\ S_a(0) = 0.30,\ E_a(0) = 0.05,$$
$$I_a(0) = 0.02,\ R_a(0) = 0.03,\ S_v(0) = 0.50,\ E_v(0) = 0.20,\ I_v(0) = 0.10.$$

Baseline parameter values are listed in Table 4. We simulate for $\alpha \in \{0.85, 0.90, 0.95, 1.00\}$ to assess memory effects.

Table 4: Baseline parameter values used in numerical simulations.

Parameter	Value	Unit
λ_h	0.000045	day^{-1}
λ_e	0.000030	day^{-1}
λ_v	0.071	day^{-1}
μ_h	0.000045	day^{-1}
μ_v	0.071	day^{-1}
γ_e	0.10	day^{-1}
γ_a	0.08	day^{-1}
γ_v	0.20	day^{-1}
α_e	0.05	day^{-1}
α_a	0.04	day^{-1}
Ω_a	0.01	day^{-1}
Υ	0.50	bites·mosquito^{-1}·day^{-1}
φ_{ve}	0.30	dimensionless
φ_{va}	0.20	dimensionless
φ_{ev}	0.25	dimensionless
φ_{av}	0.15	dimensionless

Lower α values delay epidemic peaks and reduce peak magnitudes, as shown in Table 5. Memory effects also smooth transitions and prolong infection persistence compared to $\alpha = 1.00$.

Table 5: Peak infection levels and time-to-peak for different fractional orders α.

α	**Peak of** $I_e(t)$	**Time to Peak (days)**	**Peak of** $I_a(t)$ **/** $I_v(t)$
0.85	0.045	46	0.018 / 0.095
0.90	0.048	40	0.020 / 0.098
0.95	0.052	35	0.022 / 0.100
1.00	0.060	30	0.025 / 0.105

Figure 3 summarizes peak levels and time-to-peak trends, while Figure 4 overlays infection curves across all fractional orders.

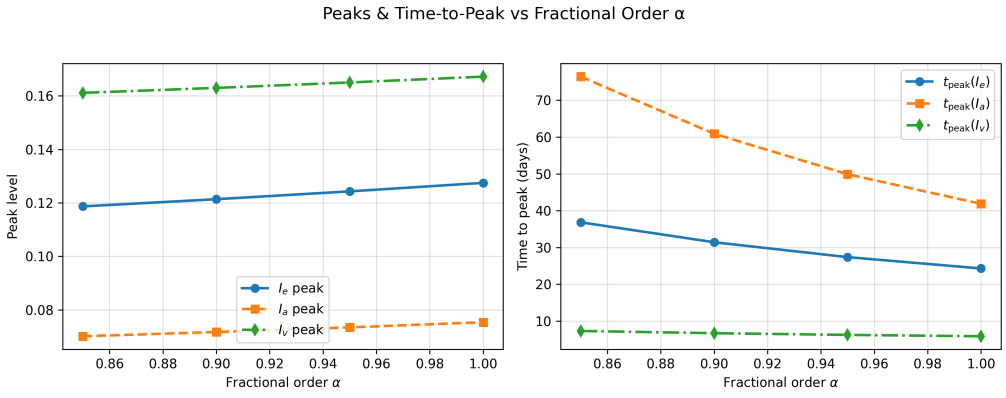

Figure 3: Variation of peak infection levels (left panel) and corresponding time-to-peak (right panel) for I_e, I_a, and I_v as α decreases from 1.00 to 0.85. Memory effects lead to smaller peaks and longer outbreak durations, highlighting the influence of fractional dynamics on malaria transmission.

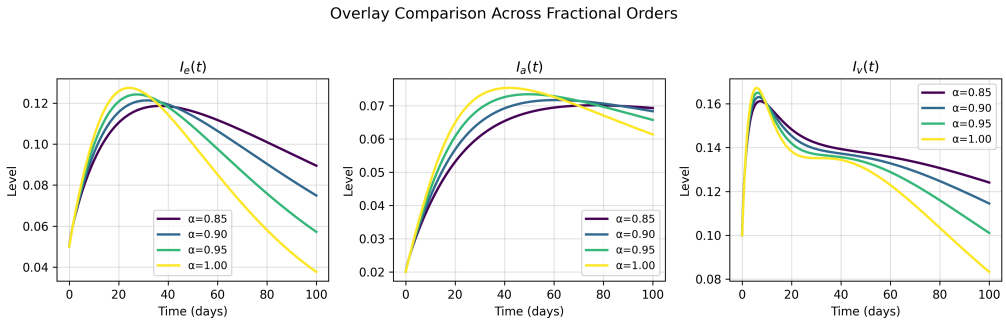

Figure 4: Overlay of $I_e(t)$, $I_a(t)$, and $I_v(t)$ trajectories for fractional orders $\alpha \in \{0.85, 0.90, 0.95, 1.00\}$. The plots illustrate smoother epidemic curves, delayed peaks, and extended persistence for lower α, confirming the role of history-dependent effects in disease dynamics.

Tables 4 and 5, together with Figures 3-4, confirm that fractional-order dynamics significantly influence malaria transmission patterns. These results support the analytical findings in Sections (7) and (8), demonstrating that memory effects slow disease progression and extend infection persistence.

11. Results and Discussion

Numerical simulations were performed for the fractional-order malaria model using the scheme described in Section (10). Baseline parameter values are listed in Table 4, and initial conditions assume normalized populations ($N_h = N_v = 1$). Fractional orders $\alpha \in \{0.85, 0.90, 0.95, 1.00\}$ were considered to assess the impact of memory effects. Figures 3-4 illustrate the time evolution of infected compartments $I_e(t)$, $I_a(t)$, and $I_v(t)$ for different α. Key observations include:

- Delayed Peaks: As α decreases, epidemic peaks occur later (e.g., t_{peak} for I_e shifts from 30 days at $\alpha = 1.00$ to 46 days at $\alpha = 0.85$).
- Reduced Peak Magnitude: Lower α values yield smaller peak infection levels (e.g., I_e^{max} decreases from 0.060 to 0.045).
- Extended Persistence: Memory effects smooth the epidemic curve, prolonging infection tails compared to the classical case ($\alpha = 1.00$).

These findings confirm that fractional dynamics capture history-dependent effects such as partial immunity and repeated exposure. Lower α values mimic stronger memory, reducing outbreak intensity but increasing duration. This aligns with analytical results (Theorems 5.7 and 5.8) and previous studies on fractional epidemiological models. Sensitivity analysis shows that variations in biting rate and infection probabilities significantly affect R_0 and peak prevalence. Control strategies targeting these parameters (e.g., insecticide-treated nets, indoor spraying) can substantially reduce R_0 and flatten epidemic curves. Finally, using the control effort metric $E = 1 - 1/R_0$ (Section (9)), the effort required to achieve $R_0 < 1$ increases with higher baseline transmission. For example, if $R_0 = 2.5$, at least 60% reduction in effective transmission is needed. Figure 2 and Table 3 illustrate this relationship, providing a quantitative basis for resource allocation in malaria control programs.

12. Conclusion

This study developed and analyzed a ten-compartment fractional-order malaria model incorporating Caputo derivatives to capture memory effects in disease dynamics. The main contributions are:

1. Formulation of a fractional-order model distinguishing non-immune and semi-immune human classes and mosquito compartments.

2. Analytical derivation of the basic reproduction number R_0 and stability conditions for disease-free and endemic equilibria.
3. Quantification of control effort required to reduce R_0 below unity.
4. Numerical simulations demonstrating that lower fractional orders delay epidemic peaks, reduce infection intensity, and extend disease persistence.

Compared to classical integer-order models, the fractional framework provides a more realistic representation of malaria transmission, especially in endemic regions where immunity and repeated exposure play critical roles. These insights can inform the design of time-sensitive intervention strategies and resource allocation for malaria control. Future research will focus on:

- Parameter estimation using real-world epidemiological data.
- Optimal control analysis incorporating cost-effectiveness of interventions.
- Extension to stochastic fractional models for uncertainty quantification.

References

[1] Ahmed, I., Tariboon, J., Muhammad, M., & Ibrahim, M. J. (2024). A mathematical and sensitivity analysis of an HIV/AIDS infection model. International Journal of Mathematics and Computer in Engineering, 3(1), 35–46. 1

[2] Aguegboh, N. S., Agbata, A., Okyere, E., Osman, S., & Andrawus, J. (2025). A novel approach to modeling malaria with treatment and vaccination as control strategies in Africa using the Atangana-Baleanu derivative. Modeling Earth Systems and Environment, 11, 110. 1

[3] Anderson, R. M., & May, R. M. (1991). Infectious diseases of humans: Dynamics and control. Oxford University Press. 1

[4] Bhatter, S., Jangid, K., Kumawat, S., Baleanu, D., Purohit, S. D., & Suthar, D. L. (2024). A new investigation on fractionalized modeling of human liver. Scientific Reports, 14(1), 1636. 1

[5] Bhatter, S., Kumawat, S., Bhatia, B., & Purohit, S. D. (2024). Analysis of COVID-19 epidemic with intervention impacts by a fractional operator. An International Journal of Optimization and Control: Theories & Applications (IJOCTA), 14(3), 261275. 1

[6] Bhatter, S., Kumawat, S., & Purohit, S. D., & Suthar, D. L. (2025). Mathematical modeling of tuberculosis using Caputo fractional derivative: a comparative analysis with real data. Scientific Reports, 15, 12672. 1

[7] Boulkroune, A., Zouari, F., & Boubellouta, A. (2025). Adaptive fuzzy control for practical fixed-time synchronization of fractional-order chaotic systems. Journal of Vibration and Control. Advance online publication. 1

[8] Boutiba, M., Baghli-Bendimerad, I. S., & Bouzara-Sahraoui, I. N. E. H. (2024). Numerical solution by finite element method for time Caputo-Fabrizio fractional partial diffusion equation. Advanced Mathematical Models & Applications, 9(2), 316–328. 1

[9] Diallo, O., Dasumani, M., Okelo, J. A., Osman, S., Sow, O., Aguegboh, N. S., & Okongo, W. (2025). Fractional optimal control problem modeling bovine tuberculosis and rabies co-infection. Results in Control and Optimization, 18, 100523. 1

[10] Diabate, A. B., Sangare, B., & Koutou, O. (2022). Mathematical modeling of the dynamics of vector-borne diseases transmitted by mosquitoes: Taking into account aquatic stages and gonotrophic cycle. Nonautonomous Dynamical Systems, 9(1), 205236. 1

[11] Diethelm, K. (2010). The analysis of fractional differential equations. Springer. 1, 5, 8

[12] Ducrot, A., & Magal, P. (2009). A mathematical model for malaria involving differential susceptibility, exposedness and infectivity of human host. Journal of Biological Dynamics, 3(6), 574598. 1

[13] Garrappa, R. (2021). Numerical solution of fractional differential equations. Mathematics, 9(11), 1272. 1, 2.6, 10

[14] Gellow, G. T., Munganga, J. M. W., & Jafari, H. (2023). Analysis of a ten compartmental mathematical model of malaria transmission. Advanced Mathematical Models & Applications, 8(2), 140156. 1, 3, 4

[15] Golmankhaneh, A. K., Welch, K., Tunç, C., et al. (2023). Classical mechanics on fractal curves. The European Physical Journal Special Topics, 232, 991–999. 1

[16] Jafari, H., Tajadodi, H., & Gasimov, Y. S. (2025). Modern computational methods for fractional differential equations. Chapman & Hall/CRC. 1

[17] Kachhia, K. B. (2023). Chaos in fractional order financial model with fractal-fractional derivatives. Partial Differential Equations in Applied Mathematics, 7, 100502. 1

[18] Khan, M. A., DarAssi, M. H., Ahmad, I., Seyam, N. M., & Alzahrani, E. (2024). Modeling the dynamics of tuberculosis with vaccination, treatment, and environmental impact: Fractional order modeling. Computer Modeling in Engineering Sciences, 141(2), 13651394. 1

[19] Khirsariya, S. R., Yeolekar, M. A., Yeolekar, B. M., & Chauhan, J. P. (2024). Fractional-order rat bite fever model: A mathematical investigation into the transmission dynamics. Journal of Applied Mathematics and Computing, 70(4), 38513878. 1
[20] Krc, Ö., Agamalieva, L., Gasimov, Y. S., & Bulut, H. (2024). Investigation of the wave solutions of two spacetime fractional equations in physics. Partial Differential Equations in Applied Mathematics, 2024, 100775. 1
[21] Kumawat, S., Bhatter, S., Bhatia, B., Purohit, S. D., Baskonus, H. M., & Suthar, D. L. (2025). Novel application of q-HAGTM to analyze Hilfer fractional differential equations in diabetic dynamics. Mathematics and Computers in Simulation, 238, 136–149. 1
[22] Kumawat, S., Bhatter, S., Bhatia, B., Purohit, S. D., & Suthar, D. L. (2024). Mathematical modeling of allelopathic stimulatory phytoplankton species using fractal-fractional derivatives. Scientific Reports, 14(1), 20019. 1
[23] Kumawat, S., Bhatter, S., Suthar, D. L., Purohit, S. D., & Jangid, K. (2022). Numerical modeling on age-based study of coronavirus transmission. Applied Mathematics in Science and Engineering, 30(1), 609–634. 1
[24] Li, X., Chen, Y. and Podlubny, I. (2010). Mittag-Leffler stability of fractional order nonlinear dynamic systems. Computers & Mathematics with Applications, 59(5), 18101821. 8
[25] Macdonald, G. (1957). The epidemiology and control of malaria. Oxford University Press. 1
[26] Mangongo, Y. T., Bukweli, J.-D. K., Kampempe, J. D. B., & Munganga, J. M. W. (2025). Mathematical model of malaria transmission dynamics: Evaluating the impact of asymptomatic and resistant strains in human hosts. Advanced Mathematical Models & Applications, 10(3), 648674. 1
[27] Manohara, G., & Kumbinarasaiah, S. (2024). Numerical approximation of fractional SEIR epidemic model of measles and smoking model by using Fibonacci wavelets operational matrix approach. Mathematics and Computers in Simulation, 221, 358396. 1
[28] Matignon, D. (1996). Stability results for fractional differential equations with applications to control processing. Computational Engineering in Systems Applications, 2(1), 963968. 1, 8, 8, 8
[29] Meena, M., Purohit, M., Shyamsunder, S. D., Purohit, S. D., Baleanu, D., & Suthar, D. L. (2024). A novel fractionalized investigation of tuberculosis disease. Applied Mathematics in Science and Engineering, 32(1), Article 2351229. 1
[30] Osman, S., Diallo, O., Dasumani, M., Andrawus, J., Sow, O., & Aguegboh, N. S. (2024). Modeling the transmission routes of hepatitis E virus as a zoonotic disease using fractional-order derivative. Journal of Applied Mathematics, 2024, Article 5168873. 1
[31] Öztürk, Z., Bilgil, H., & Sorgun, S. (2024). Fractional SAQ alcohol model: stability analysis and Türkiye application. International Journal of Mathematics and Computer in Engineering, 3(2), 125–136. 1
[32] Shyamsunder, S. D., Purohit, S. D., & Suthar, D. L. (2024). A novel investigation of the influence of vaccination on pneumonia disease. International Journal of Biomathematics, Article ID 2450080. 1
[33] Tirite, G., & Suthar, D. L. (2025). A mathematical model for analyzing the spread of Malaria. International Journal of Biomathematics. Advance online publication. 1
[34] Ullah, S., Khan, M. A., & Farooq, M. (2018). A fractional model for the dynamics of TB virus. Chaos, Solitons & Fractals, 116, 6371. 1
[35] Zhang, X. H., Ali, A., Gul, T., Khan, A., & Alshomrani, A. S. (2021). Mathematical analysis of the TB model with treatment via Caputo-type fractional derivative. Discrete Dynamics in Nature and Society, 2021, Article 9512371. 1